EDMS No. 338177

EUROPEAN ORGANIZATION FOR NUCLEAR RESEARCH
European Laboratory For Particle Physics

CERN-TIS-2002-002-RP

NEUTRON PRODUCTION FROM 158 GeV/c PER NUCLEON LEAD IONS ON THIN COPPER AND LEAD TARGETS IN THE ANGULAR RANGE 30º – 135º

S. Agosteo [1,2], C. Birattari [2,3], A. Foglio Para [1], L. Gini [2],
A. Mitaroff [4], M. Silari [4] and L. Ulrici [4]

(1) Dipartimento di Ingegneria Nucleare, Politecnico di Milano, via Ponzio 34/3, 20133 Milano, Italy.
(2) Istituto Nazionale di Fisica Nucleare, Sezione di Milano, via Celoria 16, 20133 Milano, Italy
(3) Università degli Studi di Milano, Dipartimento di Fisica, via Celoria 16, 20133 Milano, Italy.
(4) CERN, 1211 Geneva 23, Switzerland.

Abstract

The neutron emission from 5, 10 and 20 mm thick lead and 10 and 20 mm thick copper targets bombarded by a lead ion beam with momentum of 158 GeV/c per nucleon were measured at the CERN Super Proton Synchrotron. The neutron yield and spectral fluence per incident ion on target were measured with an extended range Bonner sphere spectrometer in the angular range 30º – 135º with respect to beam direction. Monte Carlo simulations with the FLUKA code were performed to establish a guess spectrum for the unfolding of the experimental data. The results have shown that, lacking Monte Carlo radiation transport codes dealing with ions with masses larger than one atomic mass unit, a reasonable prediction can be carried out by scaling the result of a Monte Carlo calculation for protons by the projectile mass number to the power of 0.85 to 0.95 for a lead target and 0.88 to 1.03 for a copper target.

Submitted for publication in Nuclear Instruments and Methods B

CERN, 1211 Geneva 23, Switzerland
13 February 2002

1. Introduction

Data on neutron emission from the interaction of heavy ion beams with matter are far less abundant in the literature than data on neutron production from protons. Systematic measurements of yield and energy distribution of neutrons produced by the interaction with various targets of ion beams from carbon to xenon with energy of up to 800 MeV per nucleon were recently published by Kurosawa et al. [1-3]. On the contrary, data on neutron production from ultra-relativistic heavy ion beams are very scarce. Such data are important to establish source terms for shielding calculations of high-energy ion accelerators. This is also in view of the fact that the various Monte Carlo codes applicable for radiation protection calculations, such as FLUKA [4-7], MCNPX [8] and MARS [9], do not treat secondary particle production from ions with masses larger than one atomic mass unit. Development work is under way to implement ion transport in FLUKA, but the new version of the code has not yet been released.

There is a general lack of knowledge about the source terms for neutron production from high-energy heavy ions. Measurements of the spectral fluence and the ambient dose equivalent of secondary neutrons produced by 250 GeV/c protons and 158 GeV/c per nucleon lead ions were recently performed at CERN around a thick beam dump [10]. These measurements showed that the spectral fluence of the secondary neutrons outside a thick shield is similar for light (protons) and heavy (lead) ions of comparable energy per nucleon stopped in a thick target. It was also shown that the approach of considering a high-energy lead ion as an independent grouping of free protons is sufficiently accurate for the purpose of evaluating the ambient dose equivalent of secondary neutrons outside thick shielding. The neutron yield from lead ion beams dumped in a thick target appears to depend on energy as [11, 12]:

$$Y \propto E_{Pb}^{0.8} \tag{1}$$

where E_{Pb} is the energy per nucleon of the ions. The yield also appears to scale linearly with the mass number of the projectile.

While in a massive dump the development of the hadronic cascade results in a variation of the neutron yield with energy as given above, with a thin target the high-energy cross-sections vary much slower and are roughly equal to their geometrical values [13]. Preliminary measurements of the neutron emission from a thin lead target bombarded by beams of high-energy protons/pions and lead ions were discussed in a previous paper [14]. Measurements were performed of the neutron yield and spectral fluence at 90° from a relatively thin (20 mm thick and 20 mm in diameter) lead target bombarded by a beam of either high-energy mixed protons/pions or lead ions. A comparison between Monte Carlo simulations and experimental data allowed the determination of a scaling factor, found to be the ratio of the experimental yield measured with lead ions to that simulated with a proton beam of the same energy per nucleon. This scaling factor allows one to calculate the neutron yield for lead ions from the results of a Monte Carlo simulation for a proton beam of the same energy per nucleon. It was found that the scaling factors depend only weakly on the beam energy and a value of $A^{0.84}$ can be used conservatively in the range of 40-160 GeV/c.

Following these preliminary results, further measurements were planned to extend these data to different target materials and a wider angular range. The present paper discusses measurements performed with lead ions employing an improved Bonner Sphere Spectrometer (BSS) with extended response function and a new experimental apparatus.

The neutron yield and spectral fluence from 5, 10 and 20 mm thick lead and 10 and 20 mm thick copper targets bombarded by a beam of $^{208}Pb^{82+}$ lead ions at 158 GeV/c per nucleon was measured at CERN in one of the secondary beam lines of the Super Proton Synchrotron (SPS). The neutron emission per incident ion on target was measured in the angular range from 30° to 135° with respect to the beam direction. Since as mentioned above the available Monte Carlo codes do not treat secondary particle generation from primaries with mass larger than one atomic mass unit, simulations with the FLUKA code were only performed to establish a guess spectrum for the unfolding of the experimental data. The experimental details are given in section 2; section 3 discusses the Monte Carlo simulations, whilst section 4 describes the spectrum unfolding procedure applied to the experimental data. The experimental results are discussed in section 5.

2. Experimental

As for the previous experiment [14], the measurements were performed in the experimental area used by the NA57 [15, 16] and ALICE [17] collaborations, in one of SPS secondary beam lines in the North Experimental Area on the Prevéssin site of CERN. Since in the first experiment only very limited beam time could be allocated to these measurements, a new experimental apparatus was built equipped with remotely controlled multiple target holder and detector support. In this way the measurements were conducted in a purely parasitic mode during the normal running of NA57. Access to the experimental area was thus only needed to change the Bonner sphere every 36 measurements (see below). The system was installed in the same position as in the previous experiment, i.e. a few metres downstream of the NA57 apparatus, on a concrete platform normally employed by the ALICE collaboration. The zone is laterally and top shielded by 80 cm concrete. One of the detectors used normally by one of the experiments was employed as beam monitor, i.e. a Cherenkov quartz detector counting pulses from individual particles, installed about 2 m upstream of the target.

The experimental device (Figure 1) consists of a supporting frame (A) over which a fan-shaped platform (B) slides horizontally, perpendicularly to the beam axis, to position the target holder in and out of the beam.

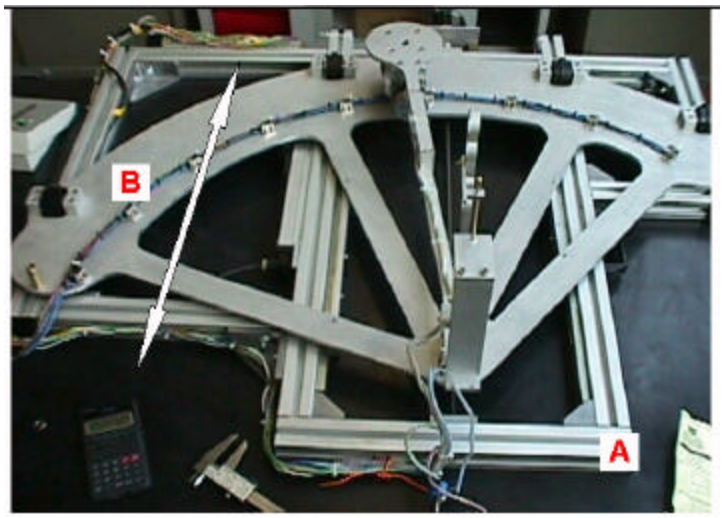

Fig. 1. The experimental device used for the neutron spectrometry measurements, allowing the semiautomatic positioning of target and detector.

An arm, with the detector support at its end, moves on the platform swinging around the target holder. The target to detector distance is 600 mm, which permits a good angular resolution of the measurement yet keeping the device compact. Four targets with diameter of up to 25 mm can be mounted on the holder (Figure 2), but one position is left empty for background measurements. The holder moves vertically to position the selected target in the beam. The target holder has a vertical excursion of 126 mm and a positioning accuracy of better than 0.1 mm. Its position is determined by a rotative transducer fitted to a worm screw driven by a stepping motor. A CsI scintillator coupled to a photodiode is mounted at the centre of the holder. This scintillator is used as a reference to correctly align the targets in the beam. The 150 mm horizontal excursion of the platform B is driven by a stepping motor coupled to a worm screw, with a resolution of better than 0.1 mm. The speed can be adjusted between 0.1 and 4 mm s^{-1}. The detector arm moves over an angular range of 120º in 15º steps, from 15º to 135º with respect to the beam direction. The arm is driven by a stepping motor fitted directly to a wheel (Figure 2); the positioning accuracy is 0.05º. The entire system is remotely controlled; the correct positioning of the detector arm at the various angular locations is sensed by micro-switches and indicated on the control panel by leds. The stepping motors for the three independent movements (horizontal of the platform, vertical of the target holder and angular of the detector arm) are driven by four-phase unipolar control boards of Eurocard format, operating at low voltage and installed in an Europac standard rack close to the device. The transducer signals are processed by boards installed in the same rack and sent to the control panel. The actual positions of the platform, of the detector arm and of the target holder are displayed on the control panel, from which the three movements are also controlled. The correct operation of the equipment is additionally surveyed by a video camera.

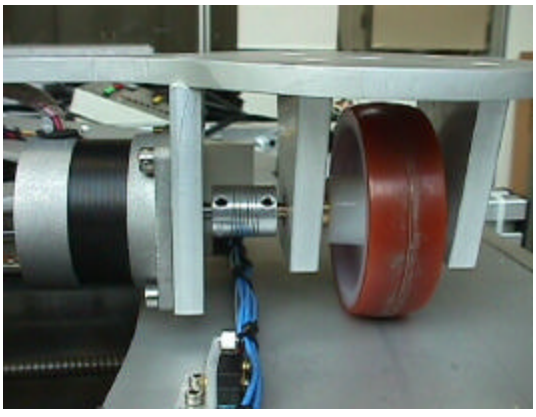

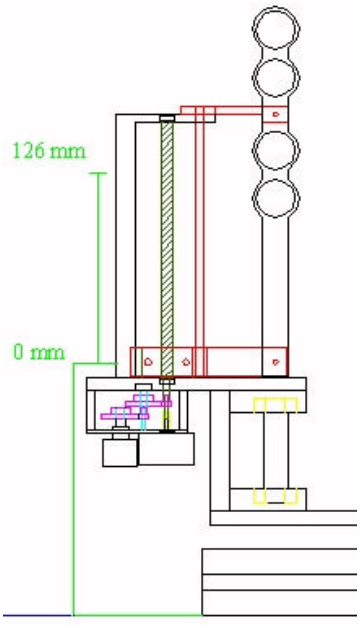

Fig. 2. Left: detail of the driving mechanism of the swinging arm for detector positioning. Right: sketch of the multiple target holder.

The neutron spectrometry measurements were performed with the 6-sphere BSS [14, 18] previously employed, integrated with two dedicated high-energy channels. The spectrometer used a Centronics ^{3}He proportional counter connected via a preamplifier to an acquisition system (amplifier, single channel analyser and counter from EG&G Ortec)

housed in a portable chassis. The proportional counter is coupled with a set of five polyethylene spheres (diameter 81 mm, 108 mm, 133 mm, 178 mm and 233 mm) plus two newly designed for the evaluation of the neutron component above 15 MeV [19]. The sphere with diameter 81 mm was also exposed with a cadmium cover. As in the previous measurements, the extended range neutron rem counter LINUS [20-23] was also employed as an additional high-energy channel. This makes a total of nine BSS detectors.

Of the two new Bonner spheres, the first (nicknamed "Ollio") is a sphere with a diameter of 255 mm and consists of moderator shells of (from the central ^{3}He proportional counter outwards) 3 cm polyethylene, 1 mm cadmium, 1 cm lead and 7 cm polyethylene thickness. This configuration suppresses the response to incident neutrons with energies lower than 100 keV and increases it for energies above 10 MeV and up to 1 GeV, as compared to the 233 mm sphere of our conventional BSS. However the response function still shows the peak at about 10 MeV which is typical for all large detectors of a BSS. The second detector ("Stanlio"), with a diameter of 118.5 mm, consists of moderator shells of 2 cm polyethylene, 1 mm cadmium and 2 cm lead thickness. Its response function does not show the peak at 10 MeV, so that Stanlio is a useful complement to the other detectors. At low energies it behaves like a small Bonner sphere, but at high energies the response is increased compared to the 233 mm sphere. The response functions of the various detectors are given in ref. [19].

Measurements without target were performed with each detector for background subtraction. The background is generated by interaction of the beam with upstream components (although the overall thickness of the material present in the beam path is small), by radiation scattered from the local shielding and the dump (situated approximately 20 m downstream of the target) and by interaction with air. The interaction length for lead ions in air is about 55 m (versus 750 m for protons), so that in the 20 m air path upstream of the target the interaction probability is about 30%.

The remote-control multiple target holder and detector arm of the experimental apparatus allowed to perform 36 measurements, namely 9 angles and four target positions (three targets plus background) with each detector of the BSS. Access to the experimental area was only required to change detector, thus keeping to a minimum any interference with the data taking of NA57. The count rate was sufficiently high that the statistical uncertainties on the single measurements was always below a few percent (and often less than 1%). Data at 15º had to be discarded because all measurements at this angle showed a large low-energy component in the reaction charged particle spectra of the ^{3}He counter. This component is most likely due to gamma radiation generated by the interaction of the beam halo with the moderator (polyethylene or polyethylene/lead) of the Bonner sphere. This component distorted the particle spectrum to such an extent as to introduce a too large uncertainty in the neutron counts. An increased low-energy component in the spectrum is also present at 30º with respect to larger angles, although not so large to jeopardise the data. Nevertheless, the results at this angle may be affected by a somewhat larger error with respect to data at 45º-135º.

3. Monte Carlo simulations

The Monte Carlo simulations were performed with the FLUKA code [4-7]. The spectral fluence of secondary neutrons generated by 158 GeV/c protons striking 20 mm thick copper and lead targets was scored in void spheres with diameter 133 mm (corresponding to that of one of the Bonner spheres used for the measurements) placed at the same positions used in the experiment (i.e., at angles of 30°, 45°, 60°, 75°, 90°, 105°,

120°, 135°). The calculated spectra were used as pre-information for unfolding the experimental data. The 5 and 10 mm targets were not simulated, since the shape of the energy distribution of the secondary neutrons generated from the same materials is very similar and is adjusted by the unfolding algorithm.

Separate simulations were performed considering only the target and reproducing strictly the geometry of the concrete structure which shields locally the experimental set-up. This allowed to estimate part of the contribution of the scattered neutrons. A detailed treatment of the diffused component would have requested the simulation of all the interactions of the primary beam upstream of the target, the contribution of other experiments running in parallel and of the beam dump placed about 20 m downstream of the target. The complexity of the geometry of some structures upstream of the target together with their large distance from the scoring positions are difficult to simulate and make almost impossible to converge to sufficiently accurate results without using variance reduction techniques. Some structures (such as the beam dump) were considered in a set of simulations previously described [14], showing that, as expected the local concrete shield is responsible for most of the scattered neutrons contributing to the spectral fluence at the scoring positions.

The calculated spectral fluence of neutrons produced at 135° from a lead target bombarded by protons is shown in Figure 3. Two peaks can be observed, according to the different steps of the intranuclear cascade model. The high-energy peak is due to direct hadron-nucleon reactions and pre-equilibrium emission, while the peak at about 3 MeV comes from evaporation neutrons. It should be noted that the high-energy peak of the secondary neutrons generated by 158 GeV/c protons (calculated with FLUKA and used as pre-information for unfolding the lead ion data) is lower than that from lead ions with the same energy per nucleon.

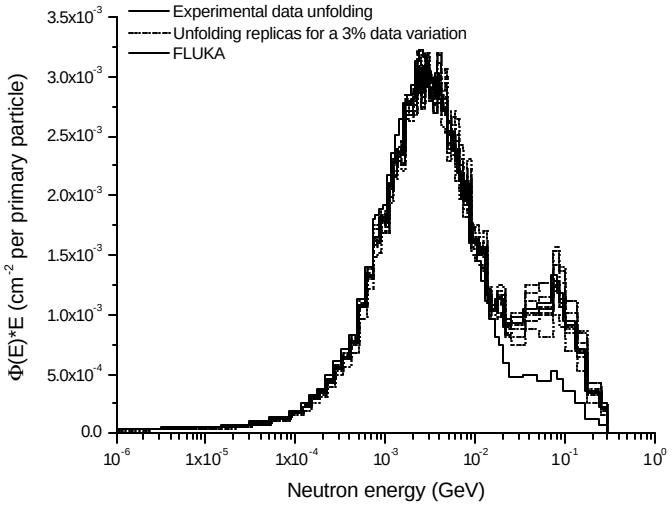

Fig. 3. Neutron spectral fluence per primary ion at 135° from 158 GeV/c per nucleon lead ions on a 20 mm thick lead target, obtained with the extended BSS (nine detectors). Lower curve (solid line): Monte Carlo guess. Upper curves: unfolding (heavy solid line) and 9 replicas (dotted lines) obtained by intentionally varying the experimental data (normal variations, 3% of mean value).

4. Spectrum unfolding

The unfolding of the data obtained with the set of nine Bonner spheres was performed with a code based on the GRAVEL formalism [24]. The code employs the MATLAB capabilities for the I/O of data and results and for the graphical presentation of other relevant quantities (e.g. chi-square, total fluence, dose, etc.) during the iterations, thus allowing a better understanding of the evolution of the procedure, as described elsewhere [14]. Since two high-energy channels were added to the set of seven Bonner spheres previously used [14], some attention was here devoted to assess the improvements of the new system versus the old one.

The response functions of the two new spheres are about twice higher than that of the LINUS, thus improving the statistics of the system under the same experimental conditions. The effect of this improvement was investigated by performing separate data unfolding with the old and the new set of detectors and the same pre-information (the simulated spectra). A marked variation of the high-energy peak was observed in the spectral fluences calculated with the complete system of nine spheres. It can thus be stated that the superior accuracy at high energies of the new BSS reduces the influence of the guess spectrum on the unfolding procedure.

The sensitivity of the unfolded spectra against the statistical fluctuations of the experimental data was checked by randomly varying the experimental counts of the Bonner spheres according to a normal distribution with a standard deviation of 3%. The results are shown in Figure 3. Particularly, the neutron fluences in large energy groups (the 4 groups of the Tables 1-5, see below) vary from 3% up to 12% for each group. These variations may be considered as a lower limit of the total uncertainties, which can be estimated as lower than 20% in each of these energy groups, if all other sources of errors are reasonably taken into account. The total fluences are obviously more stable. The behaviour of the fluences at the various angles support these considerations.

The stability of the resulting spectral fluences appears to be higher below 1MeV. The fluctuations with the new and the old BSS in the case of the lead target are compared in Figures 3 and 4, the latter referring to data unfolding with the previous set of seven Bonner spheres. With the new BSS the high-energy peak is more pronounced.

Table 1 – Neutron yield from 158 GeV/c per nucleon Pb ions on a 20 mm thick Pb target (neutrons per primary particle per steradian). The last column gives the scaling factor for a proton beam of the same energy per nucleon impinging on the same target.

Energy interval						Scaling factor (A=208)
Angle (deg)	<100 keV	0.1 - 20 MeV	20 - 300 MeV	0.3 – 2 GeV	Total	
30	6.84	36.33	48.03	17.51	108.71	$A^{0.95}$
45	5.43	34.15	35.92	3.69	79.19	$A^{0.91}$
60	4.98	33.85	24.37	0.55	63.74	$A^{0.88}$
75	4.87	32.52	17.66	0.13	55.18	$A^{0.86}$
90	4.45	31.16	14.05	0.12	49.78	$A^{0.86}$
105	3.89	30.28	12.38	0.04	46.59	$A^{0.85}$
120	3.89	29.80	10.70	0.007	44.40	$A^{0.85}$
135	3.69	29.95	8.45	0.005	42.09	$A^{0.86}$

Table 2 – Neutron yield from 158 GeV/c per nucleon Pb ions on a 10 mm thick Pb target (neutrons per primary particle per steradian).

Energy interval					
Angle (deg)	<100 keV	0.1 – 20 MeV	20 - 300 MeV	0.3 – 2 GeV	Total
30	1.52	10.99	22.42	8.90	43.83
45	1.36	10.66	13.53	1.35	26.90
60	1.62	10.51	8.57	0.18	20.89
75	1.53	9.60	6.64	0.05	17.82
90	1.19	8.87	4.86	0.04	14.95
105	1.08	8.85	4.31	0.012	14.26
120	0.87	9.07	3.39	0.002	13.34
135	1.17	9.35	2.89	0.002	13.41

Table 3 – Neutron yield from 158 GeV/c per nucleon Pb ions on a 5 mm thick Pb target (neutrons per primary particle per steradian).

Energy interval					
Angle (deg)	<100 keV	0.1 - 20 MeV	20 - 300 MeV	0.3 – 2 GeV	Total
30	0.50	3.58	9.54	4.03	17.65
45	0.46	3.32	5.58	0.61	9.97
60	0.60	3.35	3.20	0.07	7.22
75	0.56	3.01	2.40	0.017	6.00
90	0.29	2.75	1.77	0.014	4.82
105	0.36	2.77	1.39	0.004	4.53
120	0.26	2.80	1.65	0.001	4.70
135	0.37	3.00	1.01	0.0005	4.38

Table 4 – Neutron yield from 158 GeV/c per nucleon Pb ions on a 20 mm thick Cu target (neutrons per primary particle per steradian). The last column gives the scaling factor for a proton beam of the same energy per nucleon impinging on the same target.

Energy interval						Scaling factor (A=208)
Angle (deg)	<100 keV	0.1 -20 MeV	20 - 300 MeV	0.3 – 2 GeV	Total	
30	2.92	12.66	38.01	22.56	76.15	$A^{1.03}$
45	2.37	12.51	23.27	4.84	42.98	$A^{0.96}$
60	2.28	12.02	14.93	1.40	30.63	$A^{0.93}$
75	1.99	11.33	10.58	0.58	24.48	$A^{0.90}$
90	1.74	10.56	7.96	0.25	20.50	$A^{0.88}$
105	1.63	10.14	6.45	0.10	18.32	$A^{0.88}$
120	1.86	9.79	5.94	0.06	17.65	$A^{0.89}$
135	1.56	9.74	5.07	0.04	16.42	$A^{0.89}$

Table 5 – Neutron yield from 158 GeV/c per nucleon Pb ions on a 10 mm thick Cu target (neutrons per primary particle per steradian).

Energy interval					
Angle (deg)	<100 keV	0.1 - 20 MeV	20 - 300 MeV	0.3 – 2 GeV	Total
30	0.75	3.92	15.72	7.83	28.22
45	0.60	3.60	9.59	1.19	14.98
60	0.71	3.58	5.25	0.13	9.67
75	0.59	3.22	3.63	0.03	7.47
90	0.37	2.95	2.55	0.023	5.89
105	0.44	2.93	1.77	0.005	5.13
120	0.33	2.74	2.03	0.001	5.11
135	0.45	3.06	1.29	0.001	4.80

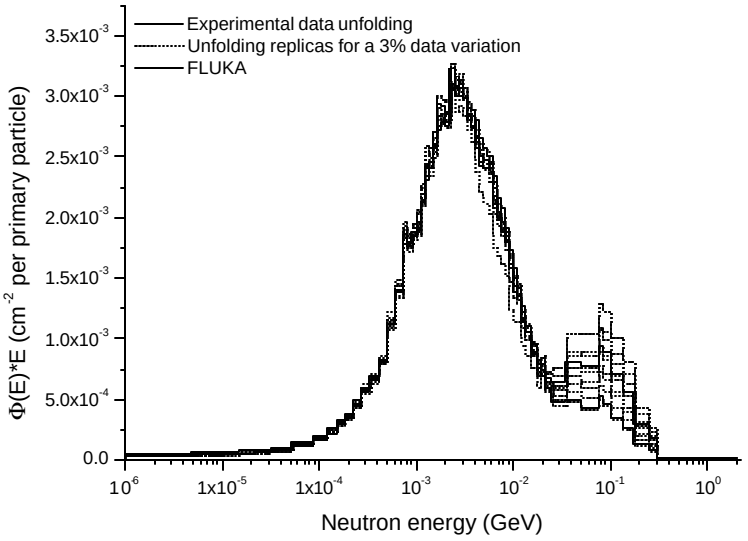

Fig. 4. Same as for Figure 3, but the neutron spectral fluence is obtained with the former BSS (seven detectors) without the two high-energy channels.

5. Results and discussion

The neutron spectral fluences for the 20 mm thick lead and copper targets are shown in Figures 5 and 6 at angles of 45°, 75°, 105° and 135°. The spectra show the two peaks predicted by the Monte Carlo guess, the isotropic evaporation component centered at 3 MeV and the high-energy peak sitting around 100-150 MeV. It should be noted that the relative importance of the high-energy peak over the evaporation peak is larger for the copper target. The energy distributions from the 5 and 10 mm thick targets are similar.

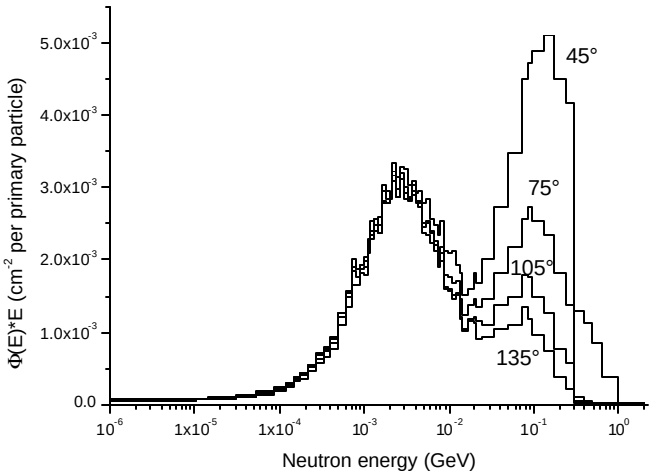

Fig. 5. Neutron spectral fluence per primary ion from 158 GeV/c per nucleon lead ions on a 20 mm thick lead target, at emission angles of (top to bottom) 45°, 75°, 105° and 135°.

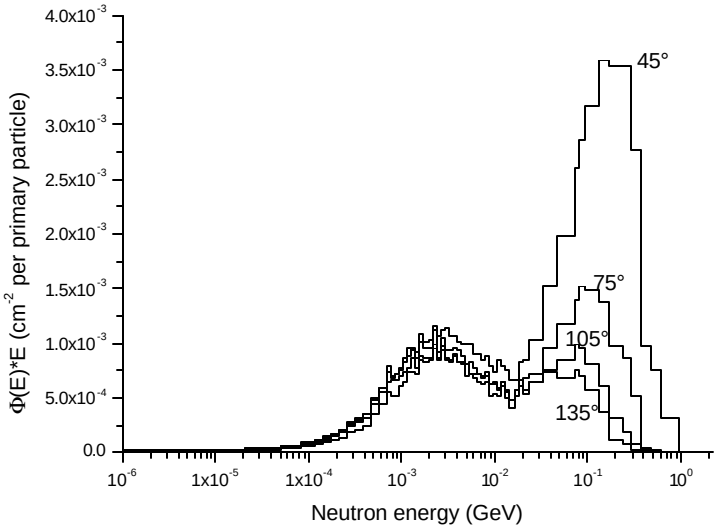

Fig. 6. Neutron spectral fluence per primary ion from 158 GeV/c per nucleon lead ions on a 20 mm thick copper target, at emission angles of (top to bottom) 45°, 75°, 105° and 135°.

The neutron yields resulting from the unfolding of the experimental data are listed in Tables 1-5 for the various target materials and thickness (5, 10, 20 mm lead and 10, 20 mm copper). The results are given in four energy bins and in the angular range 30°-135°. The results at 15° were discarded because, as explained above, the measurements were perturbed by secondary particles other than neutrons. The variation of the yield per energy group versus angle is shown in Figures 7 and 8 for the 20 mm thick lead and copper targets. The variation of the integral yield versus angle is shown in Figure 9 for all targets. The contribution of the high-energy component at the forward angles is clearly visible.

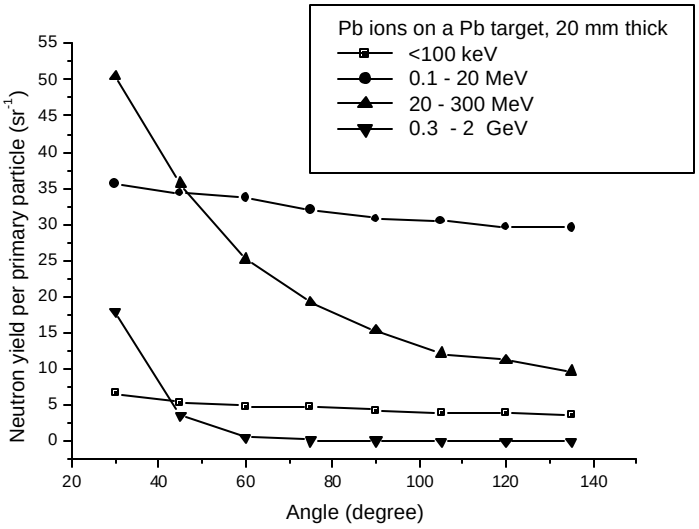

Fig. 7. Neutron yield per energy group as a function of emission angle for 158 GeV/c per nucleon lead ions on a 20 mm thick lead target.

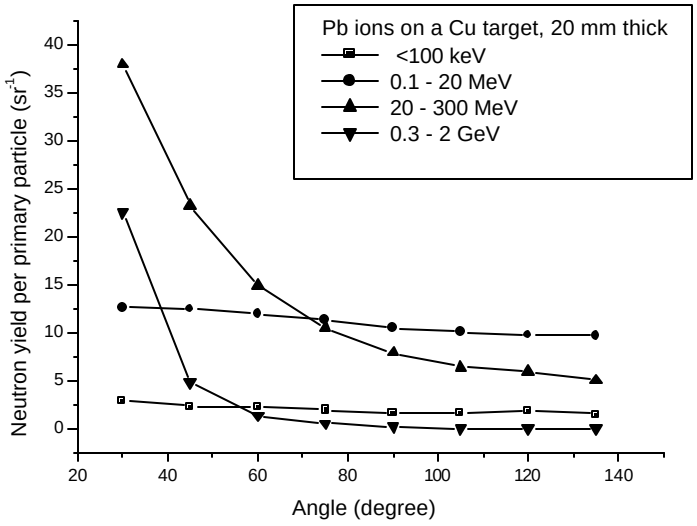

Fig. 8. Neutron yield per energy group as a function of emission angle for 158 GeV/c per nucleon lead ions on a 20 mm thick copper target.

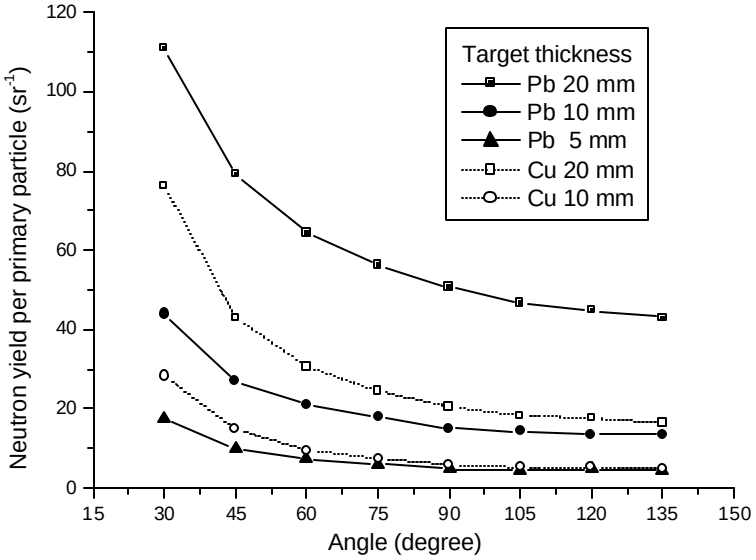

Fig. 9. Neutron yield as a function of emission angle for 158 GeV/c per nucleon lead ions on 5, 10 and 20 mm thick lead and 10 and 20 mm thick copper targets.

The scaling factors of the neutron yields with the projectile mass number are given in Tables 1 and 4, for the 20 mm thick lead and copper targets. These data were calculated by scaling the results of Monte Carlo simulations for primary protons with those from measurements with a lead ion beam (A=208) of the same energy per nucleon on the same target. The value for the 20 mm thick lead target at 90° is in good agreement with the figure $A^{0.84}$ found in the previous measurements [14]. However, it should be mentioned that this scaling law has not been proven to hold for other projectiles.

The power in the scaling law decreases from 30° to 60° and tends to a constant value at larger angles. This trend may be explained by the increase of the neutron yield with decreasing angle, due to the forward peaked distribution of the high-energy (above about 10 MeV) component of the spectral fluence. It should be noted that the power in the scaling law at the various angles is higher for the copper target than for lead. In other words, the ratio of the neutron yield for a lead ion beam on copper to that of protons striking the same material is higher than that for a lead target. This behaviour is mainly ruled by the geometrical cross-sections of the interactions.

The geometrical cross-section of an ion with mass A_{ion} (A_{ion} >1) impinging on a target with mass number A_{targ} is:

$$\sigma_{ion \to target} = \pi r_0 \left(A_{ion}^{1/3} + A_{targ}^{1/3} \right)^2 \qquad (2)$$

where r_0 = 1.3-1.5x10^{-15} m. The geometrical cross-section of a proton striking a target with mass number A_{targ} is:

$$\sigma_{p \to target} = \pi r_0 A_{targ}^{2/3} \qquad (3)$$

The ratio of the geometrical cross-sections for protons and lead ions on copper and lead is:

$$\frac{\sigma_{Pb\to Cu} / \sigma_{p\to Cu}}{\sigma_{Pb\to Pb} / \sigma_{p\to Pb}} = 1.53 \qquad (4)$$

explaining the trend of the scaling law mentioned above. The ratio of the experimental yields (lead ions on lead and lead ions on copper) to those simulated with FLUKA for a proton beam resulted to be 1.53 at 30°, 1.32 at 60° and about 1.20 at larger angles. It should be underlined that the values calculated with expression (3) (which depends on the geometrical cross-section) and the ratio of the corresponding yields cannot be compared directly because they have to be scaled by other parameters such as the number of neutrons produced per beam particle (multiplicity). Moreover, the targets used in the present experiment are not infinitely thin but rather "semi-thick".

The ratio of the geometrical cross-sections of lead ions on a lead target to that of the same projectile on copper is 1.43. The ratios of the corresponding experimental yields are in the range 1.45-2.60 and 1.55-2.76 for the 10 mm and 20 mm thick targets, respectively, the lower values referring to the lower angles. These ratios rises from 30° to 75° and remains approximately constant above. Also in this case a direct comparison between the yields and the geometrical cross-sections has poor physical meaning, but it is helpful to give confidence on the trend of the experimental data.

The variation of the integral neutron yield versus target thickness is shown in Figure 10 for lead ions on lead. It should be noted that the deviation from a linear function is more pronounced at larger angles. The yield increases by a factor in the range 2.5-3.4 by doubling the target thickness. These trends are explained by the partial development of the hadronic cascade in the targets, both in the radial and in the longitudinal direction.

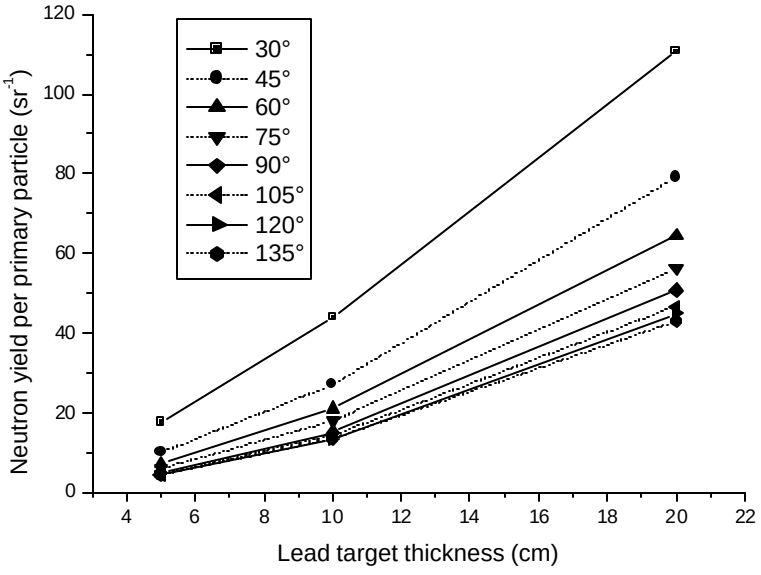

Fig.10. Neutron yield as a function of the target thickness for 158 GeV/c per nucleon lead ions on lead. The lines connecting symbols are only to guide the eye.

6. Conclusions

The results presented in this paper are the follow-up of preliminary measurements reported earlier of the neutron emission from a comparatively thin lead target bombarded by beams of high-energy protons/pions and lead ions. The neutron yield and spectral fluence from 5, 10 and 20 mm thick lead and 10 and 20 mm thick copper targets bombarded by a beam of $^{208}Pb^{82+}$ lead ions at 158 GeV/c per nucleon was here measured in the angular range from 30° to 135° with respect to the beam direction. The neutron spectral fluences show two peaks, i.e. an isotropic evaporation component centered at 3 MeV and a high-energy peak with a maximum around 100-150 MeV. It was found that the relative importance of the high-energy peak over the evaporation peak is larger for the copper target. A comparison between a Monte Carlo simulation for protons and the present experimental results for lead ions has shown that a reasonable prediction can be carried out by scaling the result of a Monte Carlo calculation for protons by the projectile mass number to the power of 0.85 to 0.95 for a lead target and 0.88 to 1.03 for a copper target. These estimates are intended to provide source term data for neutron production from high-energy heavy ions, necessary for shielding calculations and other radiation protection purposes.

Acknowledgements

The authors wish to thank F. Antinori, V. Manzari, D. Elia (NA57 collaboration) and P. Szymanski (ALICE collaboration) for allowing us to perform the measurements and for providing the beam monitoring.

References

[1] T. Kurosawa, N. Nakao, T. Nakamura, Y. Uwamino, T. Shibata, N. Nakanishi, A. Fukumura and K. Murakami, *Measurements of secondary neutrons produced from thick targets bombarded by high-energy helium and carbon ions*, Nuclear Science and Engineering 132 (1999) 30-57.

[2] T. Kurosawa, N. Nakao, T. Nakamura, Y. Uwamino, T. Shibata, A. Fukumura and K. Murakami, *Measurements of secondary neutrons produced from thick targets bombarded by high energy neon ions*, Journal of nuclear science and technology, 36 (1999) 41-53.

[3] T. Kurosawa, N. Nakao, T. Nakamura, H. Iwase, H. Sato, Y. Uwamino and A. Fukumura, *Neutron yields from thick C, Al, Cu and Pb targets bombarded by 400 MeV/nucleon Ar, Fe, Xe and 800 MeV/nucleon Si ions*, Physical Review C 62, Third series, No. 4 (2000).

[4] A. Fassò, A. Ferrari, J. Ranft and P.R. Sala, *FLUKA: present status and future developments*, Proceedings IV Int. Conference on Calorimetry in High Energy Physics, La Biodola, Italy, 21-26 September 1993, Ed. A. Menzione and A. Scribano, World Scientific (1994) p. 493-502.

[5] A. Ferrari and P.R. Sala, *The Physics of High Energy Reactions*, Proceedings of the Workshop on Nuclear Reaction Data and Nuclear Reactors Physics, Design and Safety, International Centre for Theoretical Physics, Miramare-Trieste, Italy, 15 April-17 May 1996, Eds. A. Gandini and G. Reffo, Vol. 2, World Scientific (1998) 424-532.

[6] A. Fassò, A. Ferrari, J. Ranft and P.R. Sala, *An update about FLUKA*, Proceedings 2nd Workshop on Simulating Accelerator Radiation Environments, CERN, Geneva, Switzerland, 9-11 October 1995, Ed. G.R. Stevenson, CERN Divisional Report TIS-RP/97-05 (1997) p. 158-170.

[7] A. Fassò, A. Ferrari, J. Ranft and P.R. Sala, *New developments in FLUKA modelling hadronic and EM interactions*, Proceedings 3rd Workshop on Simulating Accelerator Radiation Environments, KEK, Tsukuba, Japan 7-9 May 1997, Ed. H. Hirayama, KEK Proceedings 97-5 (1997) p. 32-43.

[8] R.E. Prael and H. Lichtenstein, *User guide to LCS: The LAHET Code System*, LA-UR-89-3014, Los Alamos National Laboratory, Los Alamos, New Mexico (1989).

[9] N.V. Mokhov, S.I. Striganov, A. Van Ginneken, S.G. Mashnik, A.J. Sierk and J. Ranft, *MARS code developments*, Proceedings of the Fourth Workshop on Simulating Accelerator Radiation Environments (SARE4), Knoxville (TN, USA), 14-16 September 1998, Ed. T. Gabriel, ORNL (1998) 87-99.

[10] S. Agosteo, C. Birattari, A. Foglio Para, M. Silari and L. Ulrici, *Neutron measurements around a beam dump bombarded by high energy protons and lead ions*, Nucl. Instrum. and Methods A 459 (2001) 58-65.

[11] A. Fassò, K. Goebel, M. Höfert, J. Ranft and G.R. Stevenson, *Shielding against high-energy radiation*, Landolt-Börnstein, Numerical Data and Functional Relationships in Science and Technology, Group 1: Nuclear and Particle Physics, Editor H. Schopper, Volume 11 (1990).

[12] R.H. Thomas and G.R. Stevenson, *Radiological safety aspects of the operation of proton accelerators*, IAEA Technical Report Series No. 283, IAEA, Vienna (1988).

[13] D.H. Perkins, *Introduction to high energy physics*, Addison-Wesley, 3rd Edition, Reading, MA, (1987) p. 134.

[14] S. Agosteo, C. Birattari, A. Foglio Para, A. Mitaroff, M. Silari and L. Ulrici, *90° neutron emission from high energy protons and lead ions on a thin lead target*, Nucl. Instrum. Meth. A (in press).

[15] V. Manzari et al., *Experiment NA57 at the CERN SPS*, J. Phys. G: Nucl. Part. Phys. 25 (1999) 473.

[16] V. Manzari et al., *Silicon pixel detectors for tracking in NA57*, Nucl. Phys. A661 (1999) 716c.

[17] The ALICE collaboration, Technical Proposal, CERN/LHC95-71 (1995).

[18] R.L. Bramblett, R.I. Ewing and T.W. Bonner, *A new type of neutron spectrometer*, Nucl. Instrum. Meth. 9 (1960) 1.

[19] C. Birattari, P. Cappellaro, A. Mitaroff and M. Silari, *Development of an extended range Bonner Sphere Spectrometer*, Proceedings of Monte Carlo 2000 – Advanced Monte Carlo for Radiation Physics, Particle Transport Simulation and Applications, Lisbon (Portugal), 23-26 October 2000, Eds. A. Kling, F. Barão, M. Nakagawa, L. Távora and P. Vaz, Springer-Verlag (2001), p.1157-1162.

[20] C. Birattari, A. Ferrari, C. Nuccetelli, M. Pelliccioni and M. Silari, *An extended range neutron rem counter*, Nucl. Instrum. Meth. A 297 (1990) 250.

[21] C. Birattari, A. Esposito, A. Ferrari, M. Pelliccioni and M. Silari, *A neutron survey-meter with sensitivity extended up to 400 MeV*, Radiat. Prot. Dosim. 44 (1992) 193.

[22] C. Birattari, A. Esposito, A. Ferrari, M. Pelliccioni and M. Silari, *Calibration of the neutron rem counter LINUS in the energy range from thermal to 19 MeV*, Nucl. Instrum. Meth. A 324 (1993) 232.

[23] C. Birattari, A. Esposito, A. Ferrari, M. Pelliccioni, T. Rancati and M. Silari, *The extended range neutron rem counter LINUS: overview and latest developments*, Radiat. Prot. Dosim. 76 (1998) 135.

[24] M. Matzke, *Unfolding of pulse height spectra: the HEPRO program system*. Braunschweig, Germany, PTB, Bericht 19 (1994).